Biosensors and Bioelectronics 35 (2012) 193–199

Contents lists available at SciVerse ScienceDirect

Biosensors and Bioelectronics

journal homepage: www.elsevier.com/locate/bios

Nanographene-based tyrosinase biosensor for rapid detection of bisphenol A

Lidong Wu [1], Dehui Deng [1], Jing Jin, Xianbo Lu *, Jiping Chen *

Dalian Institute of Chemical Physics, Chinese Academy of Sciences, Dalian 116023, China

ARTICLE INFO

Article history:
Received 21 December 2011
Received in revised form 13 February 2012
Accepted 20 February 2012
Available online 7 March 2012

Keywords:
Bisphenol A
Nanographene
Carbon nanotubes
Tyrosinase biosensor

ABSTRACT

Hydrophilic nanographene (NGP) prepared by ball milling of graphite was used as the support to construct a novel tyrosinase biosensor for determination of bisphenol A (BPA). The performances of the nanographene-based tyrosinase biosensor were systematically compared with those of multiwall carbon nanotubes (MWNTs) modified tyrosinase biosensors. The results indicated that the nanographene-based tyrosinase biosensor provided significant advantages over MWNTs-based tyrosinase biosensor in term of response, repeatability, background current and limit of detection (LOD), which could be attributed to its larger specific surface area and unique hierarchical tyrosinase-NGP nanostructures. The nanographene-based tyrosinase biosensor displayed superior analytical performance over a linear range from 100 nmol L^{-1} to 2000 nmol L^{-1}, with LOD of 33 nmol L^{-1} and sensitivity of 3108.4 mA cm^{-2} M^{-1}. The biosensor was further used for detecting BPA (leaching from different vessels) in tap water, and the accuracy of the results was validated by high performance liquid chromatography (HPLC). The nanographene-based tyrosinase biosensor proved to be a promising and reliable tool for rapid detection of BPA leached from polycarbonate plastic products and for on-site rapid analysis of emergency pollution affairs of BPA.

1. Introduction

Bisphenol A (BPA) is an organic compound with two phenol functional groups, which is extensively used to make polycarbonate plastic (PC) and epoxy resins, along with other applications. BPA has been widely disseminated within the environment during manufacturing processes or by leaching from commercial PC products (Vom Saal and Myers, 2008). Recently, BPA leaching from PC baby bottle led to negative health effects for infants, which had attracted public attention. Concerns about the usage of BPA in consumer products were regularly reported since 2008 after several governments questioned its safety, and prompted some retailers to remove products containing it from their shelves (Sanchez-Acevedo et al., 2009; Wan et al., 2010). Especially, Canada and China declared BPA as a toxic substance and banned the use of BPA in baby bottles from September 2010 and March 2011, respectively. As an endocrine disrupting chemical (EDC), BPA could mimic the body's own hormones, lead to negative health effects and increase risk of cancer (Melzer et al., 2008; Sonnenschein and Soto, 2010). In recent years, the high frequent environmental accidents resulting from BPA have been considered as one of the most fundamental concerns in global society. Thus, it is essential to develop a rapid, reliable, sensitive and high-selective method for determination of BPA.

Conventional analytical techniques for BPA determination are mainly high performance liquid chromatography (HPLC), HPLC-MS (Schug et al., 2011) and gas chromatography-mass spectrometry (GC–MS) (Altamirano et al., 2011). These analytical techniques can achieve high sensitivity and good precision, but these techniques have to be operated by highly trained technicians, and require time-consuming sample pretreatment, making them unsuitable for on-site rapid monitoring. Biosensors are ideally alternative analytical tools for on-site monitoring environmental pollutants (Song et al., 2011a; Wu et al., 2011). Amongst biosensors, the enzyme biosensor has received great attention due to its simplicity, sensitivity and selectivity for monitoring environmental pollutants. Besides, the enzyme biosensor possesses low cost and minimal requirement for sample pretreatment.

As is well known, biosensing materials play a vital role in the development of enzyme biosensor (Lu et al., 2009). The superior biosensing material is the core technology of enzyme biosensor for improving enzymatic catalysis activity and stability in vitro, limit of detection (LOD) and sensitivity, etc. Recently, Kong and Gu groups had developed electrochemical tyrosinase biosensors based on palygorskite–expanded graphite (Kong et al., 2010) and ZnO nanorods (Gu et al., 2009) for determination of phenolic pollutants with LOD of 4.5 μM and 623 nM, respectively. However, widespread application of tyrosinase biosensor for monitoring phenolic pollutants was still limited by the insufficient LOD and

* Corresponding authors. Tel.: +86 411 84379562; fax: +86 411 84379562.
E-mail addresses: xianbolu@dicp.ac.cn (X. Lu), chenjp@dicp.ac.cn (J. Chen).
[1] The authors contribute equally to this work.

0956-5663/$ – see front matter © 2012 Elsevier B.V. All rights reserved.
doi:10.1016/j.bios.2012.02.045

low enzymatic catalysis activity and stability. As a novel carbon nanomaterial, graphene possesses high specific surface area, good electric conductivity, excellent chemical and thermal stability, high mechanical strength and toxicological safety, which opens up a good prospect for the application in enzyme biosensor (Liu et al., 2012, 2011; Song et al., 2011b). While pure graphene is hydrophobic (the strong hydrophobic nature makes it tend to agglomerate in aqueous solution) and has poor dispersion in aqueous solution (Loh et al., 2010), which severely restricts its application in biosensor. Compared with previously reported hydrophobic graphene (Wang et al., 2009; Zeng et al., 2010), hydrophilic nanographene was prepared by simple ball milling of graphite in this work, which held abundant hydroxyl and carboxyl (about 8.4%) on its defect sites and edges (Deng et al., 2011), and possessed well dispersion in aqueous solution. Its sufficient hydroxyl and carboxyl functional groups were also favorable for enzyme attachment via electrostatic interactions and hydrogen bond interaction, and provided a biocompatible microenvironment for tyrosinase to keep their stability and bioactivity.

The as-prepared unique nanographene material was used as an enzyme immobilization platform and electrode material to construct an electrochemical tyrosinase biosensor for BPA. Meanwhile, the performances of nanographene-based tyrosinase biosensor were systematically compared with those of MWNTs-based tyrosinase biosensors. It indicated that the nanographene-based tyrosinase biosensor exhibited faster response, better operation repeatability, higher sensitivity, lower background current and LOD than MWNTs-based tyrosinase biosensor. These desirable electrochemical performances of nanographene-based tyrosinase biosensor were attributed to its larger specific surface area and unique layer-by-layer self-assembly (LBL) immobilization mode of enzyme molecules.

2. Materials and methods

2.1. Materials

BPA was obtained from Alfa Aesar China (Tianjin) Co., Ltd. Chitosan (Chi) and tyrosinase (from mushroom, >1000 units mg^{-1}, pI 5.92) were purchased from Sigma. MWNTs (purity > 95%) were obtained from the Chengdu Institute of Organic Chemistry (China). Acetonitrile was HPLC grade from Fisher Company. All other chemicals (analytical grade) were purchased from Tianjin Kermel Chemical Regent Company. 50 mmol L^{-1} phosphate buffer solutions (PBS, pH 7.0) were prepared by mixing standard solutions of K_2HPO_4 and KH_2PO_4. Unless otherwise mentioned, PBS (50 mmol L^{-1}, pH 7.0) was used as the electrolyte in all experiments. Milli-Q water (18 MΩ cm) was used throughout all experiments.

2.2. Apparatus

Transmission electron microscope (TEM) images were obtained with a transmission electron microscope JEM-2000EX (JEOL, Japan) with an accelerating voltage of 300 kV. Nitrogen adsorption–desorption isotherms were obtained on a Micromeritics ASAP 2010 apparatus at −196 °C. Before the measurements, the samples were degassed at 180 °C for 6 h. The specific surface areas were calculated by Brunauer–Emmett–Teller (BET) method. Fourier Transform Infrared (FTIR) spectra were obtained from a Spectrum GX spectrometer (PerkinElmer Company, USA). High performance liquid chromatography (HPLC) analyses were conducted on an Agilent 1200 HPLC with a fluorescence detector.

Electrochemical impedance spectroscopy (EIS) measurements were performed in a 2 mmol L^{-1} $K_3[Fe(CN)_6]/K_4[Fe(CN)_6]$ (1:1) solution containing 0.1 mol L^{-1} KCl, and the results were plotted in the form of complex plane diagrams (Nyquist plots) with a frequency range from 0.1 Hz to 10 kHz. Cyclic voltammetry and current–time curve (*I*–*t*) were carried out on glassy carbon (GC) electrodes (diameter, 3 mm) using an Electrochemical Workstation (CHI 440B, USA). The measurements were based on a three-electrode system with the tyrosinase-based GC electrode as the working electrode, an Ag/AgCl electrode (KCl concentration: 3 mol L^{-1}) as the reference electrode, and a platinum wire as the auxiliary electrode.

2.3. Preparation of nanographene

Nanographene was synthesized by a ball milling method according to our previous report (Deng et al., 2011). In a typical experiment, 2.0 g graphite powder and 60 g steel balls (1–1.3 cm in diameter) were put into a hardened steel vial inside a glove box and purged with high purity argon (99.999%) for 20 min before the vials were sealed. The ball milling was carried out at 450 rpm for 20 h to yield nanographene sheets.

2.4. Construction of tyrosinase biosensor

The nanographene modified tyrosinase biosensor was prepared by a simple casting method. First, the surface of GC electrode was mechanically polished by alumina powder with a diameter of 0.05 μm, and washed ultrasonically by Milli-Q water and ethanol, respectively. Then, the surface of electrode was dried with purified nitrogen stream. To obtain good performance, the mass ratios of nanographene, tyrosinase and chitosan in solution were optimized in control experiments. The final compositions of nanographene, tyrosinase and chitosan in solution were 0.4 mg mL^{-1}, 2.5 mg mL^{-1} and 1.5 mg mL^{-1}, respectively. The preparation process was as follows: Firstly, 10 μL tyrosinase (10 mg mL^{-1}) was added into 20 μL nanographene aqueous solution (0.8 mg mL^{-1}), and the mixture solution was shaking for 1 h. Then, 10 μL 6 mg mL^{-1} chitosan (chitosan, a linear polysaccharide with good film-forming ability) was injected into the above solution. Finally, 4 μL of the above mixture was cast onto the freshly polished surface of GC electrode. A beaker was covered over the electrode so that water could be evaporated slowly and a uniform film electrode was formed. The dried electrode (denoted as Tyr-NGP-Chi/GC) was stored at 4 °C in a refrigerator until in use.

Other enzyme electrodes were prepared with the similar procedures as described above. The suspension containing 0.4 mg mL^{-1} MWNTs, 2.5 mg mL^{-1} tyrosinase and 1.5 mg mL^{-1} chitosan was used to prepare the Tyr-MWNTs-Chi/GC electrode, the suspension containing 2.5 mg mL^{-1} tyrosinase and 1.5 mg mL^{-1} chitosan was used to prepare the Tyr-Chi/GC electrode, the suspension containing 0.4 mg mL^{-1} nanographene and 1.5 mg mL^{-1} chitosan was used to prepare the NGP-Chi/GC electrode, and the solution containing 1.5 mg mL^{-1} chitosan was used to prepare the Chi/GC electrode. Before electrochemical measurements, all the tyrosinase-based electrodes were stirred in 50 mmol L^{-1} PBS (pH 7.0) for 30 min to remove residual mixtures.

2.5. Detection of BPA by Tyr-NGP-Chi/GC biosensor

The amperometric current–time curves for BPA were performed to comparatively study the performance of different biosensors. The measurements were performed in 8 mL stirring PBS solution with a potential value of −0.1 V at room temperature with successive addition of BPA.

Scheme S1 (see the Supplementary Information) showed the schematic drawing of the flow injection amperometric tyrosinase biosensor (FIAB) fabricated in this work, which was used for the detection of tap water samples. It consisted of a precise flow

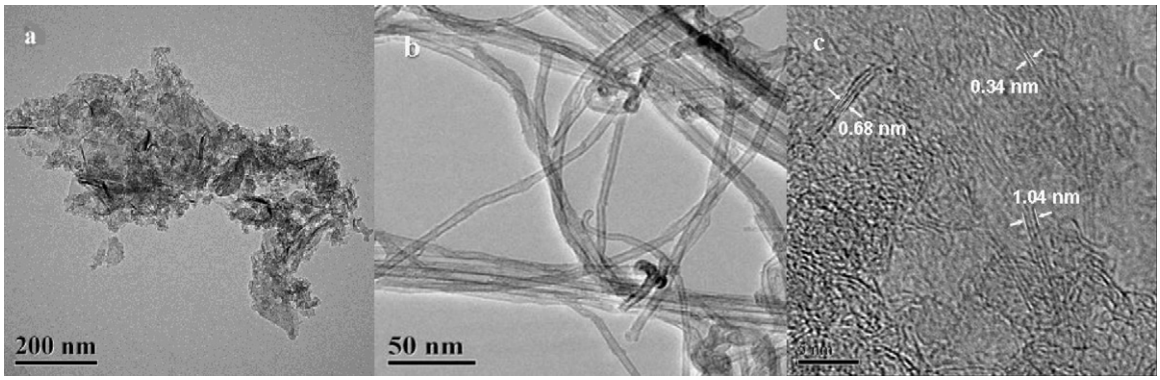

Fig. 1. TEM images of (a) nanographene, (b) MWNTs and (c) HRTEM image of nanographene.

peristaltic pump (515 Pump, HPLC, Waters), an injection valve with 800 μL injection loop, and a detection cell. The detection cell consisted of the Tyr-NGP-Chi/GC working electrode, an Ag/AgCl reference electrode, and a platinum wire auxiliary electrode. Other parts of the detection system were connected using Teflon tubing. 10 mM PBS was used as the mobile phase.

Tap water samples were obtained as follows: 60 mL tap water was added into different vessels, i.e. feeding bottle (PC, Brand A), drinking bottle (PC, Brand B), paper cup (paper, Brand C), water bottle (polyethylene glycol terephthalate (PEGT), Brand D) and glass bottle (glass, Brand E), respectively, and then the water in vessels treated by microwave heating for 10 min. These water samples without enrichment were directly injected into the FIAB system and detected by the Tyr-NGP-Chi/GC biosensor.

3. Results and discussion

3.1. Physical characterization of nanographene, MWNTs and tyrosinase–nanographene composite

Fig. 1 showed the representative TEM images of nanographene and MWNTs. As shown in Fig. 1a, nanographene obtained from pristine graphite by ball milling method displayed typical stacking structure of nanosheet. The high-resolution transmission electron microscope (HRTEM) image (Fig. 1c) indicated that high-quality single- and few-layer nanographene had been obtained by our method (Deng et al., 2011). The representative TEM image of MWNTs was displayed in Fig. 1b, with outer diameters of 10–20 nm and inner diameters of 2–5 nm, and lengths in the range of micrometres.

Specific surface area is considered as an important characteristic of nanomaterials, which can affect the immobilization of enzyme molecules. The specific surface areas of the samples were estimated by the BET method. The small-sized nanographene sheets possessed a tremendous BET specific surface area (905 $m^2\,g^{-1}$), which was significantly larger than that of MWNTs (77.6 $m^2\,g^{-1}$). The nanographene with large specific surface area provided abundant binding sites for the immobilization of tyrosinase molecules.

FTIR is a most useful tool for studying the structural changes of enzymes intercalated in the nanosheets of graphene. The fine structure of tyrosinase, nanographene and tyrosinase intercalated in nanographene (Tyr-NGP hierarchical nanocomposites) were characterized by FTIR, as shown in Fig. 2. The vibrational bands of the amide groups of tyrosinase are correlated with the secondary structure changes of this protein. The peak at 1646.9 cm^{-1} for acylamide I is the absorption of —C═O stretching vibration of peptide linkages in the protein's backbone. The peak at 1537.2 cm^{-1} for acylamide II is corresponding to the absorption of —N—H bending and C—N stretching. The positions of acylamide I and II were utilized as a "fingerprint" to identify whether tyrosinase kept its native conformation. It indicated that the absorption peaks of Tyr-NGP hierarchical nanocomposites were well matched with the characteristic absorption peaks of standard tyrosinase sample, which suggested that the immobilized tyrosinase molecules retained its native configuration even after forming novel Tyr-NGP hierarchical nanocomposites via hydrogen bond interaction and electrostatic interactions.

3.2. Electrochemical properties of nanographene modified electrodes

EIS is a very sensitive technique to monitor the formation of the adsorption layer on the GC electrode and the electron transfer reaction. The Nyquist plot of impedance spectra always includes a semicircle portion and a linear portion. The semicircle portion corresponds to the electron transfer limited process, and the linear portion corresponds to the diffusion process. And the diameter of the semicircle portion in accordance with the electron transfer limited process equals to the electron transfer resistance (Rct) (Sagara et al., 1990). In the case of a very fast electron transfer process, the Nyquist plot contains only a line portion, while an extremely slow electron transfer process includes only a large semicircle portion. Fig. 3 showed the EIS diagrams of the bare GC, Chi/GC, NGP-Chi/GC and Tyr-NGP-Chi/GC electrodes in the 2 mmol L^{-1} $K_3[Fe(CN)_6]/K_4[Fe(CN)_6]$ solution containing 0.1 mol L^{-1} KCl. Fig. 3 showed that the impedance spectrum of bare GC electrode was a straight line. The lowest Rct on the bare GC electrode indicated the fastest electron transfer rate between bare electrode and $[Fe(CN)_6]^{3-/4-}$. The diameter of the semicircle for chitosan modified GC electrode (290 Ω) was larger than that of bare GC

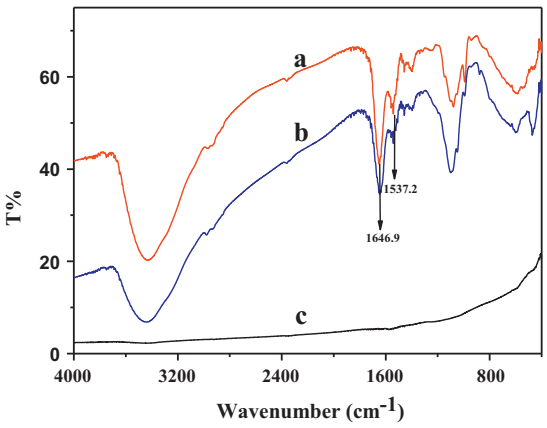

Fig. 2. FTIR spectra of (a) Tyr, (b) Tyr-NGP and (c) nanographene.

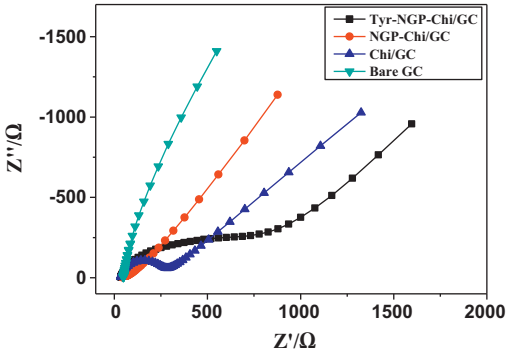

Fig. 3. Nyquist plots of bare GC, Chi/GC, NGP-Chi/GC and Tyr-NGP-Chi/GC electrodes in 2 mmol L^{-1} $K_3Fe(CN)_6/K_4Fe(CN)_6$ (1:1) containing 0.5 mol L^{-1} KNO_3.

electrode, indicating that the chitosan film formed on the surface of GC electrode hindered the electron transfer between the redox probe of $[Fe(CN)_6]^{3-/4-}$ and the electrode surface. After the nanographene was combined with chitosan to modify GC electrode, the diameter decreased significantly. The improved interface conductivity could be attributed to the introduction of nanographene, which acted as nanoscale electrodes and promoted the direct electron transfer of $[Fe(CN)_6]^{3-/4-}$ to the surface of electrode. The Rct increased to 828 Ω after immobilization of tyrosinase molecules, which could be due to the blocking of the electron transfer by the insulation of tyrosinase. The increased Rct also indicated that tyrosinase had been effectively immobilized on the electrode.

3.3. Comparative study of tyrosinase biosensors based on nanographene and MWNTs

The possible mechanism of the detection of bisphenol A based on nanographene modified tyrosinase biosensor has been illustrated in Scheme 1c. As shown, BPA (4,4′-(1-methylethylidene)bisphenol) was hydroxylated to the corresponding phenol (e.g. 4,4′-(1-methylethylidene)bis(1,2-benzoquinone)) in the presence of tyrosinase (Guix et al., 2010). Subsequently, the tyrosinase catalyzed the oxidation of the obtained polyhydric phenol to corresponding o-quinone (i.e. 4,4′-(1-methylethylidene)bis(1,2-pyrocatechol)). Finally, the obtained o-quinone could be electrochemically reduced to the corresponding polyhydric phenol for the next electrode reaction on the electrode surface. Based on the above mechanism, electrochemical tyrosinase biosensor could be used as a powerful tool for the detection of BPA. Figure S1 showed the cyclic voltammograms of the Tyr-NGP-Chi/GC electrode before and after adding BPA to PBS at 100 mV s^{-1}. After injecting 5 μmol L^{-1} BPA into 50 mmol L^{-1} PBS, an obviously increased reduction current from +0.1 V to −0.4 V was observed at Tyr-NGP-Chi/GC electrode. This indicated that the immobilized tyrosinase molecules held highly biocatalytic activity for BPA and the tyrosinase retained its bioactivity even after forming hierarchical nanocomposites of Tyr-NGP.

Amperometry is a very sensitive electrochemical method for the detection of BPA. After the optimization of working potential, −0.1 V (versus Ag/AgCl) was selected as the constant working potential for lower background current and LOD. The working potential (−0.1 V) effectively minimized the possible interference by avoiding the usage of high working potential. Fig. 4A illustrated the typical amperometric *I–t* curves of Tyr-NGP-Chi/GC (curve a), Tyr-MWNTs-Chi/GC (curve b), Tyr-Chi/GC (curve c) and NGP-Chi/GC (curve d) at −0.1 V upon successive additions of BPA standard solution to 50 mmol L^{-1} PBS under constant stirring. The NGP-Chi/GC biosensor without tyrosinase did not respond to

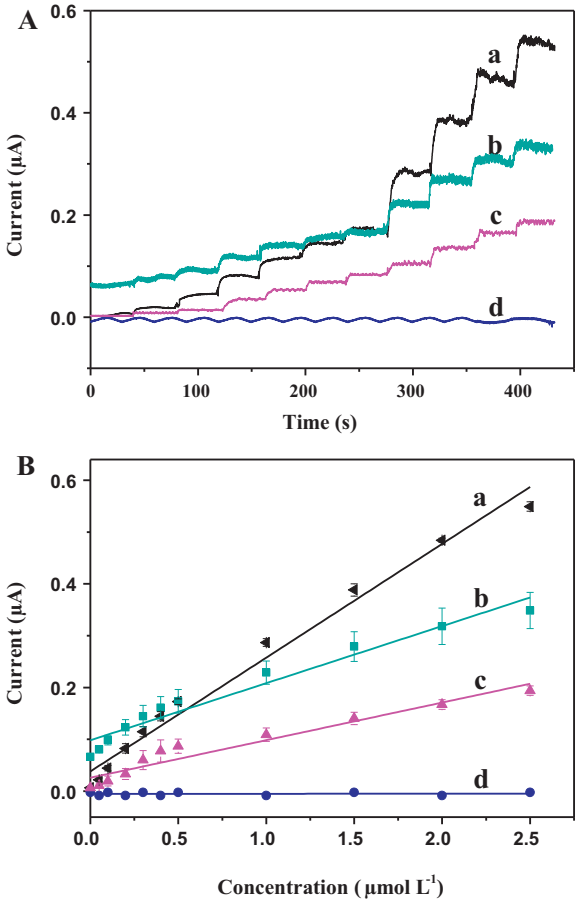

Fig. 4. (A) The typical amperometric current response curves of (a) Tyr-NGP-Chi/GC, (b) Tyr-MWNTs-Chi/GC, (c) Tyr-Chi/GC and (d) NGP-Chi/GC electrodes with successive addition of 4 μL 100 μmol L^{-1}, 8 μL 100 μmol L^{-1}, 4 μL 1 mmol L^{-1} bisphenol A into stirring 8 mL 50 mmol L^{-1} PBS (pH 7.0). Applied potential: −0.1 V versus Ag/AgCl. (B) The corresponding calibration curves of steady-state currents versus concentrations of bisphenol A: (a) Tyr-NGP-Chi/GC, (b) Tyr-MWNTs-Chi/GC, (c) Tyr-Chi/GC and (d) NGP-Chi/GC electrodes.

the changes of BPA concentrations, as shown in Fig. 4A (curve d). However, well-defined and fast amperometric signals were observed for other biosensors containing tyrosinase molecules after the addition of BPA. It indicated that tyrosinase molecules immobilized on these two carbon nanomaterial modified electrode retained their biocatalytic activity. The response time of Tyr-NGP-Chi/GC and Tyr-MWNTs-Chi/GC (achieving 95% of steady-state current) was 4 s and 6 s, respectively. The response time of Tyr-NGP-Chi/GC biosensor was faster than that of tyrosinase biosensor based on Ni nanoparticles (40 s) (Alkasir et al., 2010). Such a rapid response of Tyr-NGP-Chi/GC biosensor could be attributed to the fast diffusion of BPA from the external solution into the tyrosinase molecules immobilized on hierarchical nanostructure of graphene nanosheets (as shown in Scheme 1a). Fig. 4B showed the calibration curves of the response current of these biosensors versus the concentrations of BPA. As shown in Fig. 4B, the calibration curves of Tyr-NGP-Chi/GC, Tyr-MWNTs-Chi/GC and Tyr-Chi/GC biosensors displayed a linear relationship to BPA concentrations in the range of 100–2000 nmol L^{-1}, 300–2500 nmol L^{-1} and 400–2500 nmol L^{-1}, respectively. The sensitivity of Tyr-NGP-Chi/GC biosensor was 3108.4 mA cm^{-2} M^{-1}, which was about two times higher than that of Tyr-Chi/GC (1026.6 mA cm^{-2} M^{-1}). This indicated that nanographene could significantly improve the sensitivity of tyrosinase-based biosensor for BPA detection. Besides, the sensitivity of Tyr-NGP-Chi/GC biosensor was much higher than that of Tyr-MWNTs-Chi/GC (1557.3 mA cm^{-2} M^{-1}). The

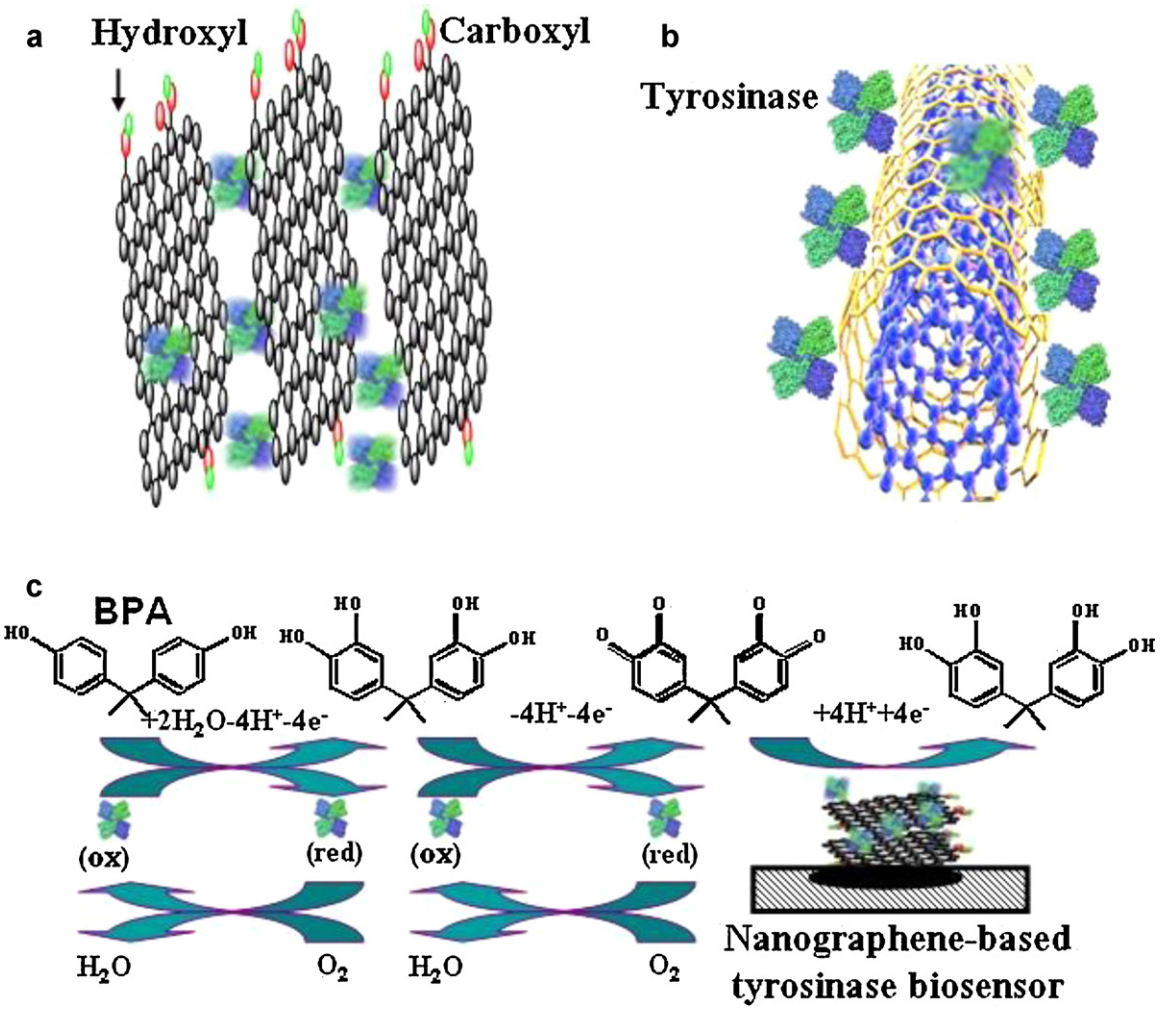

Scheme 1. Schematic diagram of tyrosinase immobilized on (a) nanographene, (b) MWNTs, (c) the mechanism of the detection of bisphenol A by the nanographene-based tyrosinase biosensor.

inter-electrodes relative standard deviation (RSD) of Tyr-NGP-Chi/GC biosensor and Tyr-MWNTs-Chi/GC biosensor were 3.4% and 9.8% at 1 μmol L^{-1} of BPA, respectively. This demonstrated the repeatability of the Tyr-NGP-Chi/GC biosensor was better than that of Tyr-MWNTs-Chi/GC biosensor.

As a biosensor, one of the most important performances of the biosensor was the LOD, which was used for "alarm" whether BPA was present in real water samples. The LOD of Tyr-NGP-Chi/GC, Tyr-MWNTs-Chi/GC and Tyr-Chi/GC biosensors were 33, 100 and 132 nmol L^{-1} at a signal-to-noise ratio of 3, respectively. The LOD of the Tyr-NGP-Chi/GC biosensor achieved 33 nmol L^{-1} (0.0075 mg L^{-1}), which was lower than the standards for drinking water quality of China (GB 5749-2006, BPA 0.01 mg L^{-1}). The Tyr-NGP-Chi/GC biosensor could be used as a reliable tool for rapid detection of BPA leaching from commercial PC products. It was evident from the above comparison that the Tyr-NGP-Chi/GC biosensor had the lowest LOD and background noise, and the highest sensitivity. Previous study revealed that the effective surface area, the structure and surface property of the nanomaterials, along with the immobilization mode of enzyme molecules could significantly influence the analytical performance of the resulting enzyme biosensor.

The good biosensing performance of the Tyr-NGP-Chi/GC biosensor can be attributed to the following aspects: firstly, the large surface area of nanographene could dramatically enlarge the active surface area of the GC electrode available for enzyme immobilization (Shan et al., 2009), which increased the surface loading quantity of tyrosinase molecules; meanwhile, those hydroxyl and carboxyl groups on the surface of nanographene provided a favorable microenvironment for the immobilization of tyrosinase via electrostatic interaction. Our previous report demonstrated that 8.4% of the oxygen-containing groups (i.e. hydroxyl, carboxyl, aldehyde and ketone) (Deng et al., 2011) was on the defects and edges of nanographene, which was higher than that on MWNTs (2.1%) according to the present energy dispersive X-ray analysis (EDX). These abundant oxygen-containing groups on nanographene together with its nanoscale size were very helpful for improving the dispersion in aqueous solution. This had also been evidenced by the photographs (Figure S2) via dispersions of the same concentration (0.8 mg mL^{-1}) of MWNTs and nanographene in aqueous solution. As shown in Figure S2, nanographene possessed better dispersion in aqueous solution compared to MWNTs, which resulted in the better repeatability of the Tyr-NGP-Chi/GC biosensor than that of Tyr-MWNTs-Chi/GC biosensor. Furthermore, these abundant hydroxyl and carboxyl groups were also useful for improving the stability of immobilized enzyme molecules (Zhang et al., 2010).

It was well known that the close distance between the electroactive center of enzyme molecules and the underlying electrode could facilitate the electron transfer between the enzyme molecules and the electrode. Considering the high electric conductivity of nanographene-based electrode material, we presume

Table 1
Comparison of determined concentration of bisphenol A in different water vessels by biosensor method and HPLC method.

Sample	Concentration ($\mu g\,mL^{-1}$) (Biosensor method)	Concentration ($\mu g\,mL^{-1}$) (HPLC method)	Difference[a] (%)
PC feeding bottle (Brand A)	0.66	0.58	12.9
PC drinking bottle (Brand B)	1.42	1.53	−7.7
Paper cup (Brand C)	Not detected	Not detected	
PEGT water bottle (Brand D)	Not detected	Not detected	
Glass bottle (Brand E)	Not detected	Not detected	

[a] Difference = $(\text{Biosensor}_{(\text{value})} - \text{HPLC}_{(\text{value})})/\text{HPLC}_{(\text{value})} \times 100\%$.

that the immobilized tyrosinase molecules may have a close contact with the nanographene support, as shown in Scheme 1a. Furthermore, the functional groups (i.e. hydroxyl and carboxyl) on the surface of nanographene and the "LBL" architectures of Tyr-NGP nanocomposites could provide a biocompatible microenvironment for immobilized tyrosinase molecules to retain their secondary structure, which further improved their enzymatic stability and bioactivity. As for MWNTs, the Tyr-MWNTs-Chi/GC biosensor had a rather lower sensitivity and a worse LOD than the Tyr-NGP-Chi/GC biosensor. The primary reason was elucidated as follow: As shown in Scheme 1b, due to the inner tube of MWNTs was too small (about 2–5 nm), the tyrosinase molecules (6.5 nm × 9.8 nm × 5.5 nm) (Sugiyama et al., 2006) could only be immobilized on the outer surface of MWNTs (Scheme 1b). Furthermore, MWNTs had smaller specific surface area than nanographene, which limited the content of immobilized tyrosinase on MWNTs surface, and only a small part of tyrosinase molecules could participate in the bioelectrocatalytic reaction. Compared with nanographene, the above disadvantages of MWNTs resulted in the lower sensitivity of the Tyr-MWNTs-Chi/GC biosensor. Furthermore, due to the high background current and noise of the Tyr-MWNTs-Chi/GC biosensor, it possessed a worse LOD than the Tyr-NGP-Chi/GC biosensor. Therefore, the lower LOD of Tyr-NGP-Chi/GC biosensor could be used as a more promising "alarm" tool for rapid detection of BPA than MWNTs-based biosensors.

3.4. Real sample detection using FIAB system

Scheme S1 showed the schematic drawing of the FIAB fabricated in this work, which was used for the detection of BPA leached from the commercial drinking bottle, such as tap water samples in PC products. These test samples without enrichment were directly injected into the FIAB system and detected by the Tyr-NGP-Chi/GC biosensor. As shown in Table 1, after the PC feeding bottle (Brand A) and PC drinking bottle (Brand B) were heated by microwave for 10 min, 0.66 $\mu g\,mL^{-1}$ and 1.42 $\mu g\,mL^{-1}$ of BPA were detected from tap water filled in the feeding bottle and drinking bottle by the Tyr-NGP-Chi/GC biosensor, respectively. For tap water in the paper cup (Brand C), the PEGT water bottle (Brand D) and glass bottle (as blank sample, Brand E), no BPA was detected by the Tyr-NGP-Chi/GC biosensor. This indicated that no BPA leached from the paper cup, the PEGT water bottle and the glass bottle into tap water. The detection results based on the Tyr-NGP-Chi/GC biosensor were validated by HPLC method (GB/T 23296.16-2009 for BPA). As shown in Table 1, the concentrations of BPA in the feeding bottle, the drinking bottle, the paper cup, the water bottle and the glass bottle were 0.58 $\mu g\,mL^{-1}$, 1.53 $\mu g\,mL^{-1}$, 0, 0 and 0 by HPLC method, respectively. This revealed that the biosensor-based detection method was a promising and reliable tool for the rapid detection of BPA leaching from PC and epoxy resins products.

The potential coexisting interferences were also systematically evaluated by the Tyr-NGP-Chi/GC biosensor. Phthalates, the most widely used plasticizers, always coexists with BPA in PC. The results demonstrated that the coexisting species in PC and epoxy resins products, such as dimethyl phthalate and octyl phthalate (with 100-fold concentration higher than BPA) did not interfere with detection of BPA. Besides, KNO_3, sodium citrate, sodium oxalate, urea, ethyl acetate, diethyl carbonate, acetonitrile, n-hexane, benzene, hexachlorobenzene and naphthalene (with 100-fold concentration higher than BPA) also did not produce any interfering signals. The good selectivity of the biosensor was attributed to the biocatalytic specificity of tyrosinase for BPA in PC. It should be noted that the device of tyrosinase-based biosensor was high-selective, sensitive, rapid, portable, low-cost and fitted for on-site analysis upon emergency pollution accidents of BPA. Note that phenolic chemicals (i.e. phenol) (Apetrei et al., 2011) as substrates of tyrosinase could interfere with the detection of BPA. However, this phenomenon could not occur in this study. Because these phenolic chemicals except BPA were not commonly used as plasticizer to make PC product (Yang et al., 2011). That is to say, there is no presence of other phenolic chemicals in PC product. Therefore, these phenolic chemicals have no effect on the specific usage of the biosensor for the detection of BPA leaching from commercial PC product.

4. Conclusions

In conclusion, based on nanographene, the Tyr-NGP-Chi/GC biosensor had been successfully constructed for BPA detection, and its analytical performance was systematically and comparatively studied with MWNTs-based tyrosinase biosensor. It indicated that nanographene provided significant advantages over MWNTs in achieving faster response, better repeatability, lower background current and LOD of fabricated tyrosinase biosensors, which could be attributed to its larger specific surface area and unique "LBL" immobilization mode of enzyme molecules (hierarchical Tyr-NGP nanostructures). The Tyr-NGP-Chi/GC biosensor was further used for rapid detection of BPA in tap water which leached from commercial PC products, and the accuracy of the results was validated by conventional HPLC method. The nanographene modified tyrosinase biosensor proved to be a promising and reliable tool for rapid detection of BPA leaching from PC products and epoxy resins products. It also has a great application prospect for on-site rapid analysis of emergency pollution affairs of BPA.

Acknowledgment

This work was supported by the National Natural Science Foundation of China (no. 20907051), the Knowledge Innovation Program of Chinese Academy of Sciences (no. DICP K2010C1), the Major State Basic Research Development Program of China (2009CB421602) and the Chinese Academy of Sciences Graduate Science and Technology Innovation Fund.

Appendix A. Supplementary data

Supplementary data associated with this article can be found, in the online version, at doi:10.1016/j.bios.2012.02.045.

References

Alkasir, R.S.J., Ganesana, M., Won, Y.H., Stanciu, L., Andreescu, S., 2010. Biosens. Bioelectron. 26, 43–49.

Altamirano, J.C., Fontana, A.R., de Toro, M.M., 2011. J. Agric. Food Chem. 59, 3559–3565.

Apetrei, C., Rodriguez-Mendez, M.L., De Saja, J.A., 2011. Electrochim. Acta 56, 8919–8925.

Deng, D., Yu, L., Pan, X., Wang, S., Chen, X., Hu, P., Sun, L., Bao, X., 2011. Chem. Commun. 47, 10016–10018.

Gu, B.X., Xu, C.X., Zhu, G.P., Liu, S.Q., Chen, L.Y., Li, X.S., 2009. J. Phys. Chem. B 113, 377–381.

Guix, M., Perez-Lopez, B., Sahin, M., Roldan, M., Ambrosi, A., Merkoci, A., 2010. Analyst 135, 1918–1925.

Kong, Y., Chen, X.H., Ni, J.H., Yao, S.P., Wang, W.C., Luo, Z.Y., Chen, Z.D., 2010. Appl. Clay Sci. 49, 64–68.

Liu, F., Piao, Y.X., Choi, K.S., Seo, T.S., 2012. Carbon 50, 123–133.

Liu, T., Xu, M.R., Yin, H.S., Ai, S.Y., Qu, X.J., Zong, S.S., 2011. Microchim. Acta 175, 129–135.

Loh, K.P., Bao, Q.L., Ang, P.K., Yang, J.X., 2010. J. Mater. Chem. 20, 2277–2289.

Lu, X.B., Xiao, Y., Lei, Z.B., Chen, J.P., 2009. Biosens. Bioelectron. 25, 244–247.

Melzer, D., Lang, I.A., Galloway, T.S., Scarlett, A., Henley, W.E., Depledge, M., Wallace, R.B., 2008. JAMA 300, 1303–1310.

Sagara, T., Niwa, K., Sone, A., Hinnen, C., Niki, K., 1990. Langmuir 6, 254–262.

Sanchez-Acevedo, Z.C., Riu, J., Rius, F.X., 2009. Biosens. Bioelectron. 24, 2842–2846.

Schug, K.A., Yang, S.H., Morgan, A.A., Nguyen, H.P., Moore, H., Figard, B.J., 2011. Environ. Toxicol. Chem. 30, 1243–1251.

Shan, C.S., Yang, H.F., Song, J.F., Han, D.X., Ivaska, A., Niu, L., 2009. Anal. Chem. 81, 2378–2382.

Song, J.M., Pal, S., Kim, J.Y., Park, S.H., Lim, H.B., Lee, K.H., 2011a. Environ. Sci. Technol. 45, 4460–4467.

Song, W., Li, D.W., Li, Y.T., Li, Y., Long, Y.T., 2011b. Biosens. Bioelectron. 26, 3181–3186.

Sonnenschein, C., Soto, A.M., 2010. Nat. Rev. Endocrinol. 6, 364–371.

Sugiyama, M., Matoba, Y., Kumagai, T., Yamamoto, A., Yoshitsu, H., 2006. J. Biol. Chem. 281, 8981–8990.

Vom Saal, F.S., Myers, J.P., 2008. JAMA 300, 1353–1355.

Wan, Y., Choi, K., Kim, S., Ji, K., Chang, H., Wiseman, S., Jones, P.D., Khim, J.S., Park, S., Park, J., Lam, M.H.W., Giesy, J.P., 2010. Environ. Sci. Technol. 44, 5233–5239.

Wang, Y., Li, Y.M., Tang, L.H., Lu, J., Li, J.H., 2009. Electrochem. Commun. 11, 889–892.

Wu, L.D., Lu, X.B., Jin, J., Zhang, H.J., Chen, J.P., 2011. Biosens. Bioelectron. 26, 4040–4045.

Yang, C.Z., Yaniger, S.I., Jordan, V.C., Klein, D.J., Bittner, G.D., 2011. Environ. Health Perspect. 119, 989–996.

Zeng, G.H., Xing, Y.B., Gao, J.A., Wang, Z.Q., Zhang, X., 2010. Langmuir 26, 15022–15026.

Zhang, Q.A., Qiao, Y., Hao, F., Zhang, L., Wu, S.Y., Li, Y., Li, J.H., Song, X.M., 2010. Chem. Eur. J. 16, 8133–8139.